Imaging Single Glycans

X. Wu[1,†], M. Delbianco[2,†], K. Anggara[1], T. Michnowicz[1], A. Pardo-Vargas[2], P. Bharate[2], S. Sen[1], M. Pristl[1], S. Rauschenbach[1,3,*], U. Schlickum[1,4], S. Abb[1], P.H. Seeberger[2,5,*], K. Kern[1,6,*]

[1] Max Planck Institute for Solid State Research, Heisenbergstraβe 1, 70569 Stuttgart, Germany [2] Max Planck Institute for Colloids and Interfaces, Am Mühlenberg 1, 14476 Potsdam, Germany [3] Department of Chemistry, University of Oxford, Mansfield Road, Oxford, OX1 3TA, UK [4] Institute of Applied Physics, Technische Universität Braunschweig, 38106 Braunschweig, Germany. [5] Institute for Chemistry and Biochemistry, Free University Berlin, Arnimallee 22, 14195 Berlin, Germany. [6] Institut de Physique, Ecole Polytechnique Fédérale de Lausanne, 1015 Lausanne, Switzerland [†] These authors contributed equally to this work.

Imaging biomolecules guides the understanding of their diverse structures and functions.[1, 2] Real space imaging at sub-nanometer resolution by cryo-electron microscopy has provided key insights into proteins and their assemblies.[3, 4] Direct molecular imaging of glycans, the predominant biopolymers on earth with a plethora of structural and biological functions,[5] is currently not possible.[6] Inherent glycan complexity and backbone flexibility require single molecule approaches for real space imaging. Glycan characterization often relies on a combination of mass spectrometry and nuclear magnetic resonance to provide insights into size, sequence, branching, and connectivity, and thus requires structure reconstruction from indirect information.[7-9] Here, we show direct imaging of single glycan molecules that are isolated by mass-selective, soft-landing electrospray ion-beam deposition and imaged by low temperature scanning tunneling microscopy (STM).[10] Sub-nanometer resolution allows for the visualization of glycan connectivity and discrimination between regio-isomers. Direct glycan imaging is an important step towards a better understanding of the structure of carbohydrates.

Glycans are biopolymers built from monosaccharide units connected through glycosidic bonds, with different regio- and stereochemistry. Their backbone flexibility results in a vast number of conformations. Unlike strictly linear proteins and nucleic acids, glycans can have branched primary structures that, in addition, may differ in the stereochemistry at each glycosidic linkage. Structure sensitive methods, such as ion mobility-mass

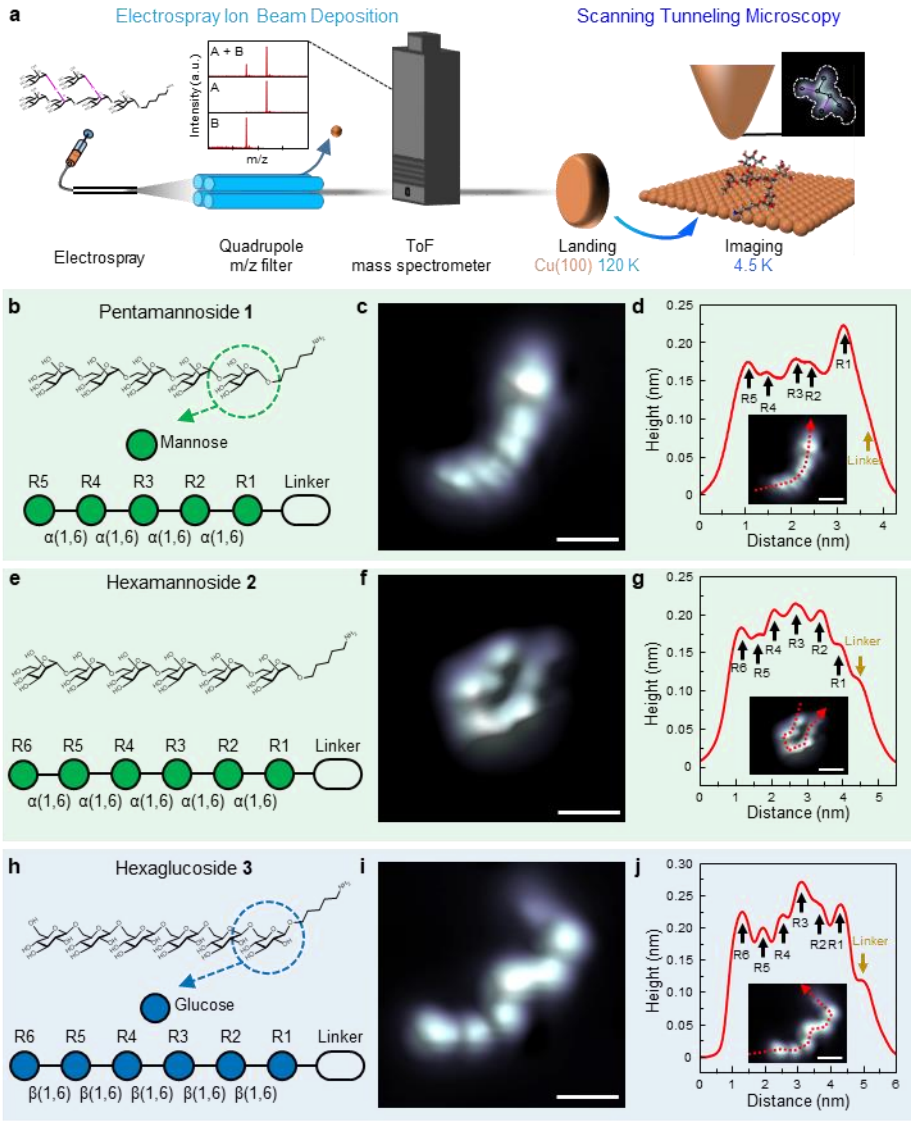

Figure 1 | STM topography imaging of linear glycans prepared by electrospray ion beam deposition. a, Schematic workflow of glycan transfer and deposition via ES-IBD combined with single glycan STM imaging in UHV. The beam is purified by mass selection in RF quadrupoles while the composition of the beam is monitored by ToF MS. The Cu (100) substrate is kept at 120 K during deposition and sample transfer. The STM is operated at 4.5 K. **b, e, and h,** Chemical structure and symbol nomenclature for glycans (SNFG) of linear α-(1→6) pentamannoside **1**, α-(1→6) hexamannoside **2**, and β-(1→6) hexaglucoside **3**, respectively. **c, f, and I,** Typical STM topography image of α-(1→6) pentamannoside **1**, α-(1→6) hexamannoside **2** and β-(1→6) hexaglucoside **3**, showing a topographic protrusion for every monosaccharide unit and a low intensity protrusion for the linker. The scale bar is 1 nm. Scanning parameters: **c,** V_s = -100 mV, I = 50 pA, **f,** V_s = -200 mV, I = 50 pA, **i**, V_s = -100 mV, I = 50 pA. **d, g, and j**, Line profile of the molecules presenting five peaks for pentamanoside (d) and six peaks for both hexamannoside (g) and hexaglucose (j) in addition to a low intensity peak of the linker.

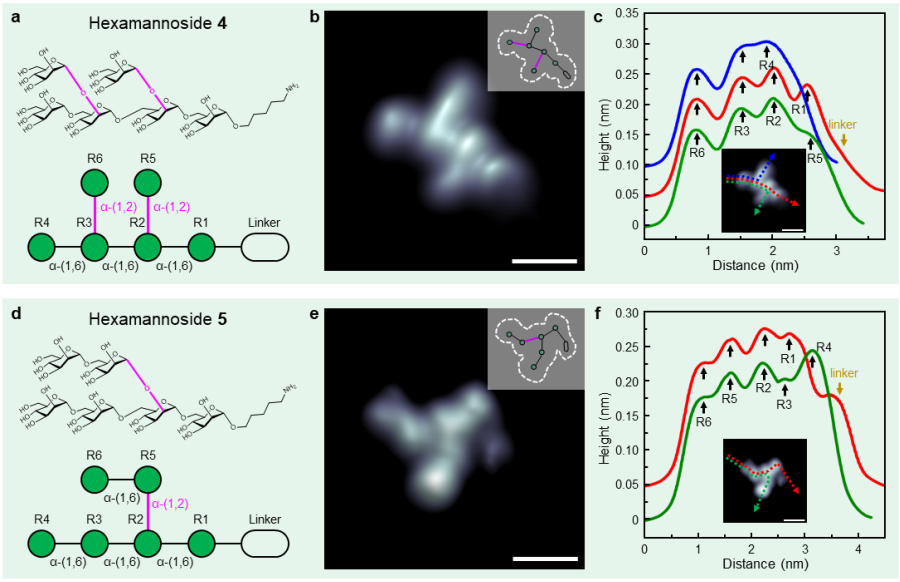

Figure 2 | STM topographic image of branched hexamanosides 4 and 5. a, d, Chemical structure and SNFG depiction of the branched hexamannosides **4** and **5**. The linkages in the backbone are all α-(1→6). The branches are connected to the backbone via α-(1→2) linkages (pink bonds). Hexamannoside **4** contains two branching points with one mannose unit per branch. Hexamannoside **5** contains one branching point consisting of two mannose units. **b, e,** Typical STM topography image of the branched hexamannosides **4** and **5**. The insets show the schematic diagrams of the conformations. The scale bar is 1 nm. Scanning parameters: **b,** V_s = -500 mV, I = 100 pA, **d,** V_s = -100 mV, I = 100 pA. **c, f,** Line profile of the molecules showing peaks for every monosaccharide unit. The different colored line profiles have an offset of 0.05 nm. The direction of the line profile is indicated in the inset.

spectrometry (IM-MS)[11] and cryo-IR spectroscopy[12] have advanced glycan analysis, taking advantage of chemically defined molecular ion beams to deliver a sample to a precise vacuum-based analysis method. These methods, however, probe structure indirectly averaging over a molecular ensemble, calling for the application of a direct imaging method such as STM.

Reliable STM experiments on a molecule require a controlled environment in ultra-high vacuum (UHV) to minimize surface impurities. Therefore, glycan samples are prepared via electrospray ion beam deposition (ES-IBD), which in tandem arrangement with STM imaging, has enabled structural analysis of numerous nonvolatile molecules, including dyes[13], proteins[14, 15], peptides[16-18], and disaccharides[19, 20]. The gas-phase, molecular ion beam of intact, non-volatile glycans (Fig. 1a) is purified by a mass-to-charge ratio (m/z) filter and monitored by time-of-flight mass spectrometry before its gentle deposition onto the atomically clean surface in UHV.[10, 21] Only a minute amount of sample, in the range of microgram, is needed for a series of sample preparations. Herein, we demonstrate that real space molecular imaging by STM can be used effectively to uncover details of the glycan structure.

Pure oligosaccharides with defined sequence and connectivity were prepared by automated glycan assembly (AGA) [22, 23] and deposited on the surface as negatively charged glycans by ES-IBD. Soft deposition conditions and thus intact deposition is ensured by selecting a low impact energy of 5eV at which covalent bonds are unaffected[19-21], whereas the conformation of a molecule can be rearranged during collision.[17] In the experiment, individual molecules on the surface are obtained by deactivating molecular diffusion on a cold surface: 120 K during deposition and 4.5 K during imaging. As a result, single molecules are observed being evenly distributed on the surface and can be distinguished from aggregates (See extended data, ED, Fig. 1ED). The ability of ES-IBD to prepare a sample with single molecules on the surface thus allows detailed structural inspection and comparison of different oligosaccharide sequences at the single molecule level.

Three linear glycans, α-(1→6) pentamannoside **1**, α-(1→6) hexamannoside **2** and β-(1→6) hexaglucoside **3**, containing an alkylamino linker group at the reducing terminus (Fig. 1b ,1e and 1h), were used for initial imaging experiments (representative images in Figure 1c, 1f and 1i, and for more images, see ED, Fig. 2ED). In a typical STM image, individual linear glycans appear of similar length at varying conformation. The cryogenic conditions can eliminate the thermal motion and the molecules are frozen in different shapes. Single monosaccharide subunits are resolved as topographic protrusions: five features for pentamannoside **1** and six features are observed for both hexamannoside **2** and hexaglucoside **3**. The heights of the individual monosaccharide features in both glycans vary between 0.15 and 0.25 nm, often clearly separated from each other by local minima (line profiles in Figs. 1d, 1g and 1j). The distances between monosaccharides, measured peak-to-peak between the topographic maxima, are 0.52±0.07 nm for all 1→6 linkages, independent of the stereochemistry (α vs β). The alkylamino linker is observed as a low height feature at one end of the molecule. With shape, size and spacing of the subunits being consistent with recent findings of STM imaging of disaccharides, we use the measured distances as indicator for different glycosidic linkages.[19, 20]

To explore whether we can distinguish between isomers with different connectivity, two branched hexamannosides, hexamannoside **4** (Fig. 2a) containing two α-(1→2) branching

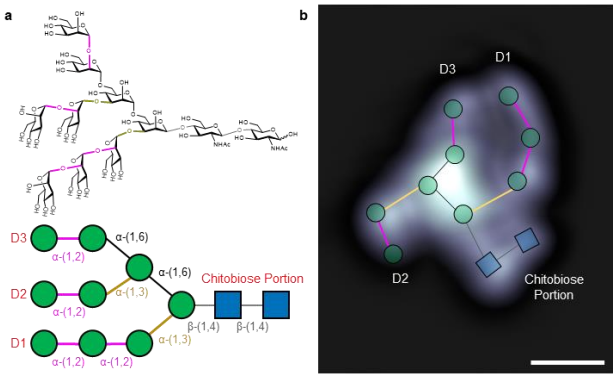

Figure 3 | STM topography image of undecasaccharide 6. a, The chemical structure and SNFG representation of undecasaccharide **6** containing eleven monosaccharide units and different linkages. **b,** Typical STM topography image of undecasaccharide **6** superimposed with the molecular structure. The assignment is performed using the number of units in one branch as well as measuring the distance between the monosaccharide units. Scanning parameters: V_s = -50 mV, I = 50 pA. The scale bar is 1 nm.

points at residues R2 and R3 and hexamannoside **5** (Fig. 2d) containing only one α-(1→2) branching point at R2, were directly imaged. Representative STM images reveal structures where branching is clearly visible (Figs. 2b and 2e, for more images, see ED, Fig. 3ED). The STM image of hexamannoside **4** shows two side chains branching out at nearly 90° angle on opposite sides of the linear backbone. Two of the measured interunit distances of 0.53±0.05 nm are assigned to the two α-(1→6) linkages. Their length is in agreement with the observation for the linear glycans. The α-(1→2) linkages appear significantly longer at 0.61±0.02 nm. This difference allows for the unambiguous assignment of the complete hexamannoside **4** (inset Fig. 2b) revealing a slight bend in the α-(1→6)-connected backbone. The interunit distance, measured peak-to-peak between the highest points in each monosaccharide, is indicated in the line profiles in Figs 2c and 2f. Because the position of the topography maximum depends on the conformation of the saccharide subunit, the distance measured from the STM typographs does not represent the exact distances of the glycosidic linkage.[19, 20] Still, the measured distance is a reliable parameter to distinguish between α-(1→2) and α-(1→6)

linkages, as for the linear glycans, the measured distances were reproduced for all investigated molecules and further matched the (1→6) distances measured for the branched glycans

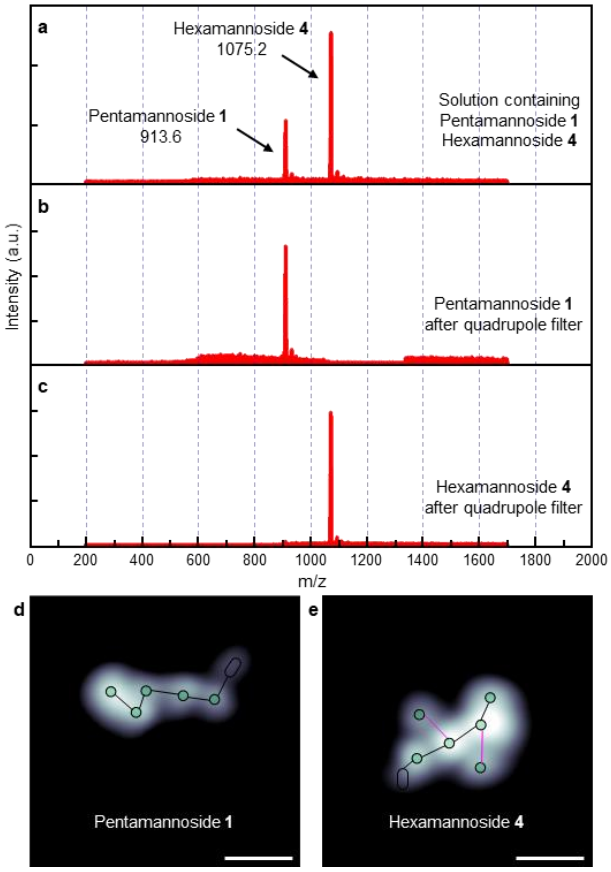

Figure 4 | Analysis of glycans from mixtures by chemically selective deposition followed by STM imaging. a, Mass spectrum of a mixture of pentamannoside **1** and hexamannoside **4**. **b,** mass spectrum of the mass filtered deposition beam only containing pentamannoside **1**. **c,** mass spectrum of the deposition beam only containing hexamannoside **4**. **d,** STM topography image of a pentamannoside **1** molecule obtained after mass filtered deposition. **e,** STM topography image of a hexamannoside **4**. STM parameters for both images: V_s = -100 mV, I = 50 pA. The scale bars are 1 nm.

(see Figs. 4ED and 5ED).

The more compact shapes observed in the STM image of hexamannoside **5** (shown in Fig. 2) are the results of the greater flexibility of this oligosaccharide. While bond rearrangement or contamination can be excluded due to the chemically selective soft-landing deposition, conformational freedom of the longer branch often impedes the direct distinction of the branching point due to 3D folding. These structures appear much higher in STM (0.3 nm) and exhibit a reduced number of protrusions in the respective single molecule image. Thus single molecule analyses were only performed on molecules for which the right number of features of correct height was found. A representative STM image of hexamannoside **5** (Fig. 2e) shows a molecule sufficiently spread to allow for the unambiguous identification of the branching point. The amino linker identifies residue R1 and thereby the position of the branching point in relation to the overall structure. The increased distance of the α-(1→2) linked branch allows for the unambiguous assignment of hexamannoside **5**.

The imaging method can be applied to more complex glycans, such as the triply-branched undecasaccharide **6** (Fig. 3). The STM image of undecasaccharide **6** shows that all branches are spread apart from each other such that each monosaccharide subunit is visible. The D1 and D2 + D3 arms can be distinguished based on the different number of mannose units. The different lengths of the α-(1→3) and the α-(1→6) linkages (0.82 and 0.53 nm, respectively) allows for the assignment of the remaining branches (D2) and (D3), thereby identifying the chitobiose branch. In the center where both 3-fold branching points are located, the molecule appears at larger height. The additional protrusion of this area, as compared to other features, can be attributed to the steric constraints imposed by three attached glycan chains.

An important advantage of this approach is the possibility of extracting specific glycans from a mixture via the mass-filtered deposition capability of ES-IBD as exemplified for a mixture of pentamannoside **1** and hexamanoside **4** (Fig. 4). The m/z filtering quadrupole is initially tuned such that only pentamannoside **1** passes, before tuning the filter window to the mass of hexamannoside **4**. STM imaging of the molecules deposited in this way reveals only structures corresponding to the selected molecules (Fig. 4 d,e).

Isolation and identification of biologically relevant glycans, even from mixtures, by the tandem-approach of preparative mass spectrometry and scanning probe microscopy imaging provides an unprecedented way to study glycan topology, structure, and function. Direct visualization of single glycans at subnanometer resolution under cryogenic conditions prevents loss of information due to conformational averaging. The mass-filtered deposition ensures that the observed geometry and topology can be unambiguously related to structural characteristics such as branching and type of linkage. This information has the potential to serve as standard for the identification of individual molecules or recurrent motifs. Unlike other techniques that provide information averaged over variable conformations and species present in a mixture, we collect data from chemically selected glycans at the single molecule level and thus can directly relate how molecular structure correlates with properties – a step forward towards cracking the "sugar code"[25].

Online content. Methods, along with any additional Extended Data display items and Source Data, are available in the online version of the

paper; references unique to these sections appear only in the online paper.

Data availability. The data that support the findings of this study are available from the authors on reasonable request, see author contributions for specific data sets.

Supplementary Information is available in the online version of the paper.

Acknowledgements. We thank the Max Planck Society and Alexander von Humboldt Foundation for financial support. M.D. thanks the Minerva Fast Track Program and the MPG-FhG Cooperation Project Glyco3Dysplay. The authors acknowledge the Emmy-Noether-Program of the Deutsche Forschungsgemeinschaft.

Author Contributions. S.R., S.A., P.H.S. and K.K. conceived this project. X.W., K.A., S.R., S.A., U.S., K.K., P.H.S., and M.D. designed the experiments. X.W., K.A., T.M., S.S., M.P., U.S. and S.A. carried out the sample preparation and measurements. X.W., S.A., T.M. analyzed the data. M.D., A.P.V., and P.B. carried out the molecule synthesis. All authors contributed to and discussed the manuscript.

Author Information. Reprints and permissions information is available at www.nature.com/reprints. The authors declare no competing financial interests. Readers are welcome to comment on the online version of the paper. Correspondence and requests for materials should be addressed to S.R. (stephan.rauschenbach@chem.ox.ac.uk), P.H.S. (peter.seeberger@mpikg.mpg.de), K.K. (k.kern@fkf.mpg.de).

Competing interests. The authors declare no competing interests.

References

1. Unwin, P. N. T.; Henderson, R. Molecular structure determination by electron microscopy of unstained crystalline specimens. *J. Mol. Biol.* **94**, 425-440 (1975).
2. Celebrating structural biology. *Nat Struct Mol Biol* **18**, 1304-1316 (2011).
3. Bai, X.-c.; McMullan, G.; Scheres, S. H. W. How cryo-EM is revolutionizing structural biology. *Trends Biochem. Sci.* **40**, 49-57 (2015).
4. Callaway, E. The revolution will not be crystallized: a new method sweeps through structural biology. *Nature* **525**, 172 (2015).
5. Varki, A., et al., *Essentials of glycobiology*. 3rd edition. Cold Spring Harbor Laboratory Press (2017).
6. Gray, C. J., et al. Advancing Solutions to the Carbohydrate Sequencing Challenge. *J. Am. Chem. Soc.* **141**, 14463-14479 (2019).
7. Mariño, K.; Bones, J.; Kattla, J. J.; Rudd, P. M. A systematic approach to protein glycosylation analysis: a path through the maze. *Nature Chem. Biol.* **6**, 713-723 (2010).
8. Dell, A.; Morris, H. R. Glycoprotein Structure Determination by Mass Spectrometry. *Science* **291**, 2351 (2001).
9. Lundborg, M.; Fontana, C.; Widmalm, G. Automatic Structure Determination of Regular Polysaccharides Based Solely on NMR Spectroscopy. *Biomacromolecules* **12**, 3851-3855 (2011).
10. Rauschenbach, S.; Ternes, M.; Harnau, L.; Kern, K. Mass Spectrometry as a Preparative Tool for the Surface Science of Large Molecules. *Annu. Rev. Anal. Chem.* **9**, 473-498 (2016).
11. Hofmann, J.; Hahm, H.; Seeberger, P.; Pagel, K. Identification of carbohydrate anomers using ion mobility-mass spectrometry. *Nature* **526**, 241 (2015).
12. Mucha, E., et al. Glycan Fingerprinting via Cold-Ion Infrared Spectroscopy. *Angew. Chem. Int. Ed.* **56**, 11248-11251 (2017).
13. Kley, C. S., et al. Atomic-scale observation of multiconformational binding and energy level alignment of ruthenium-based photosensitizers on TiO2 anatase. *Nano Lett.* **14**, 563-569 (2014).
14. Deng, Z., et al. A close look at proteins: Submolecular resolution of two- and three-dimensionally folded cytochrome c at surfaces. *Nano Lett.* **12**, 2452-2458 (2012).
15. Longchamp, J.-N., et al. Imaging proteins at the single-molecule level. *Proc. Natl. Ac. Sci.* **114**, 1474 (2017).
16. Abb, S.; Harnau, L.; Gutzler, R.; Rauschenbach, S.; Kern, K. Two-dimensional honeycomb network through sequence-controlled self-assembly of oligopeptides. *Nat. Commun.* **7**, 10335 (2016).
17. Rauschenbach, S., et al. Two-Dimensional Folding of Polypeptides into Molecular Nanostructures at Surfaces. *ACS Nano* **11**, 2420-2427 (2017).
18. Liu, L., et al. Chaperon-Mediated Single Molecular Approach Toward Modulating Aβ Peptide Aggregation. *Nano Lett.* **9**, 4066-4072 (2009).
19. Abb, S., et al. Carbohydrate Self-Assembly at Surfaces: STM Imaging of Sucrose Conformation and Ordering on Cu(100). *Angew. Chem. Int. Ed.* **131**, 8424-8428 (2019).
20. Abb, S., et al. Polymorphism in carbohydrate self-assembly at surfaces: STM imaging and theoretical modelling of trehalose on Cu(100). *RSC Adv.* **9**, 35813-35819 (2019).
21. Rauschenbach, S., et al. Electrospray Ion Beam Deposition of Clusters and Biomolecules. *Small* **2**, 540-547 (2006).
22. Guberman, M.; Seeberger, P. H. Automated Glycan Assembly: A Perspective. *J. Am. Chem. Soc.* **141**, 5581-5592 (2019).
23. Panza, M.; Pistorio, S. G.; Stine, K. J.; Demchenko, A. V. Automated Chemical Oligosaccharide Synthesis: Novel Approach to Traditional Challenges. *Chem. Rev.* **118**, 8105-8150 (2018).
24. Delbianco, M., et al. Well-Defined Oligo- and Polysaccharides as Ideal Probes for Structural Studies. *J. Am. Chem. Soc.* **140**, 5421-5426 (2018).
25. Brazil, R.: Can chemists crack the sugar code? https://www.chemistryworld.com/features/can-chemists-crack-our-cells-sugar-code/4010803.article#/.

Methods

Glycan Synthesis

AGA was performed on a home-built synthesizer developed at the Max Planck Institute of Colloids and Interfaces.[24] All details concerning pre-automation steps, building blocks, AGA modules, and post-synthesizer manipulations can be found in the SI.

Electrospray Ion-Beam Deposition

For the ES-IBD experiment, the solution of the synthesized glycans (linear pentamannoside **1**, linear hexamannoside **2**, linear hexaglucoside **6**, haxamannosides **4** and **5**) were prepared by dissolving the powder in a water-ethanol 1:1 mixture with approx. 0.1% ammonium hydroxide to result in a concentration of ~10^{-4} mol/L. For undecasaccharides **6** (GKM-002900, Prozyme), the solution was prepared with the same components in a concentration of ~10^{-5} mol/L due to the small dose (10 µg). Subsequently, negative charged gas phase ions of the glycans were generated by our home-built ES-IBD apparatus (-1 for glycans **1-5**, -2 for glycan **6**, 2-3 kV on the emitter, 20 µl/h flow rate, current up to ~200 pA, about 10 min of deposition time). Before the deposition in UHV, the composition of the ion beam is monitored by a time-of-flight (ToF) mass spectrometer and purified by RF quadrupoles. The deposition took place in the ultrahigh vacuum (UHV) chamber with a base pressure of 2×10^{-10} mbar. The landing energy of the molecular ion beam was 5 eV per charge to avoid fragmentation.

Before the deposition, the Cu (100) single crystal (Surface Preparation Laboratory, SPL) was cleaned via several cycles of Ar ion sputtering (1.2 kV, 20 min) and annealing (800 K, 10min). After the cleaning, the substrate was cooled down to ~120 K and transferred with a low temperature (LT) UHV suitcase (~120 K, 2×10^{-10} mbar) to the deposition chamber. During the deposition, the substrate was kept at ~120K.

Scanning Tunneling Microscopy

After the deposition, the sample was kept at ~120 K and transferred with the LT-UHV suitcase to the LT-STM for imaging. In all the chamber involved in the sample transfer, the base pressure is below 8×10^{-10} mbar. The STM experiments were performed in a home-built LT-STM operated at 4.5 K and

controlled by a Nanonis RC5 electronics. All voltages refer to the sample bias with respect to the tip. All STM measurements were performed with a chemical etched W tip.

Data Analysis and Statistics

STM data analysis was performed using WSxM and OriginPro 2016. Raw data was used only after a plane subtraction.

For statistical analysis single molecules were chosen from survey images and measured at high resolution, excluding clusters and agglomerations judging by size and height. The given feature distances are an average value over many distances measured. For this only molecules were taken into account where the feature height is found in the range of 0.15-0.25 nm, i.e. no clusters or 3-dimensional configurations, and where the right number of features could be resolved, which amounts to more than 80% for the linear glycans and more than 85% of the branched molecules.

For the distance of the α-(1→6) linkages in linear glycans, the statistics includes the data from 5 molecules of each linear glycan, measuring 20 linkages for Pentamannoside **1**, 25 linkages for Hexamannoside **1** and 25 linkages for Hexaglucoside **3** (see Fig. 4ED). For the distance of α-(1→2) and α-(1→6) linkages, the statistics includes 20 hexamannoside **4** molecules with 40 α-(1→6) linkages and 20 α-(1→2) linkages (see Fig 5ED).

EXTENDED DATA

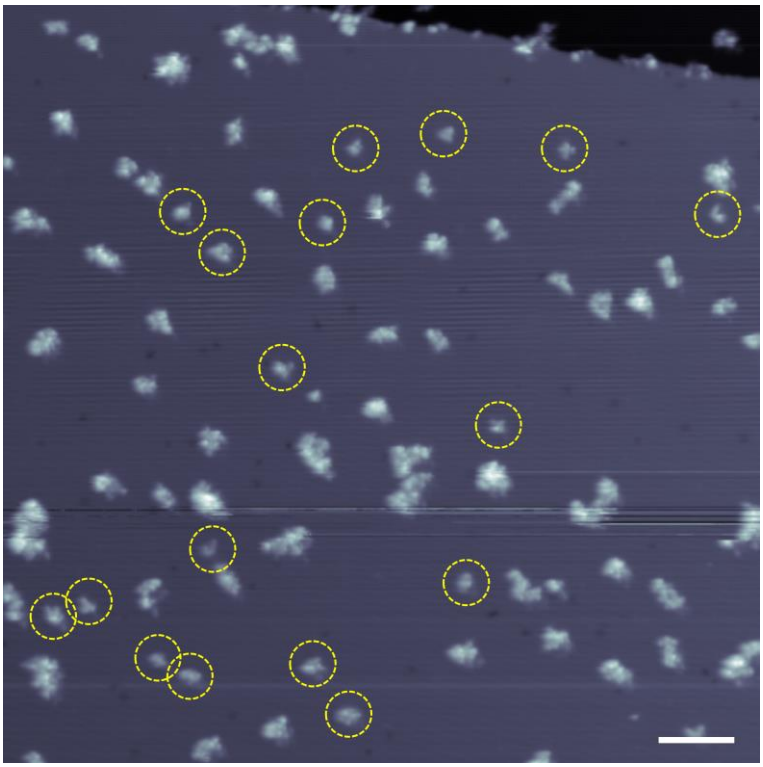

Figure 1ED | STM overview image of hexamannoside 4 sample. Single molecules (marked with yellow circles) are observed as major species on the terrace. The dark spots are due to impurities on the surface, which is typical for depositions at low temperature. Scale bar: 10 nm.

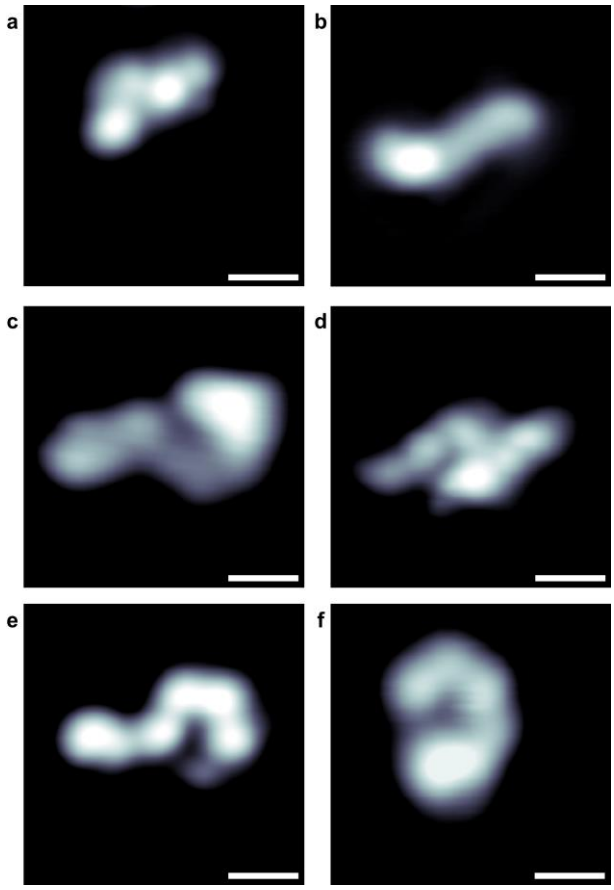

Figure 2ED | STM topography image of linear glycans. a,b STM images of pentamannoside **1** showing different conformations on the surface. **c, d** STM images of hexamannoside **2** showing different conformations on the surface. e, f, STM images of hexaglucoside **3** showing different conformations on the surface. Scale bars: 1 nm.

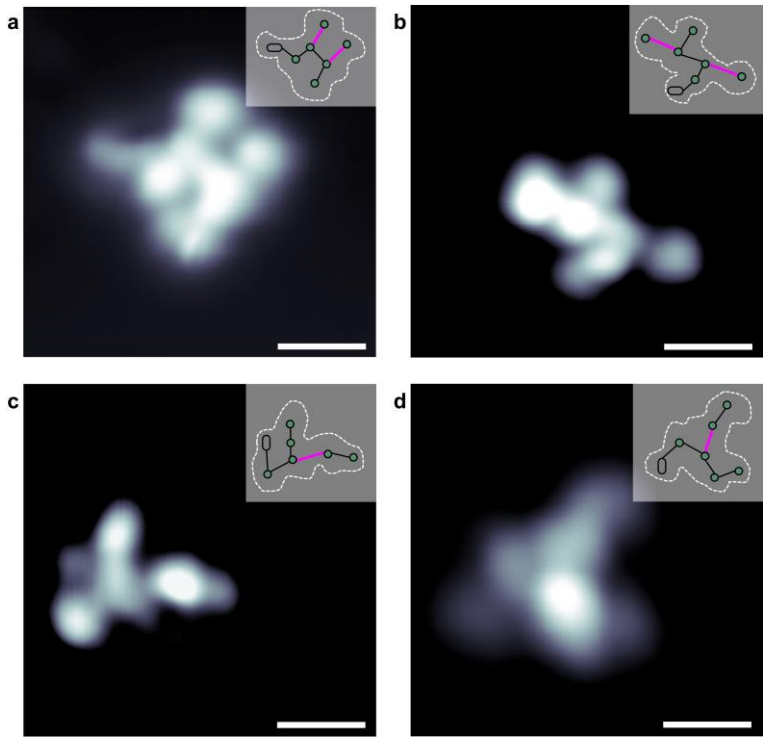

Figure 3ED | STM topography image of branched hexamannosides. a,b STM images of adsorbed hexamannoside **4** showing different conformations. Two branches are clearly visible. **c, d** STM images of hexamannoside **5** of different conformation on the surface with branching clearly visible. The assignment of the linkage is done based on the position of the linker (low height feature) and by interunit distance as assigned in the inset ((1→2) linkage in pink)**.** Scale bars: 1 nm.

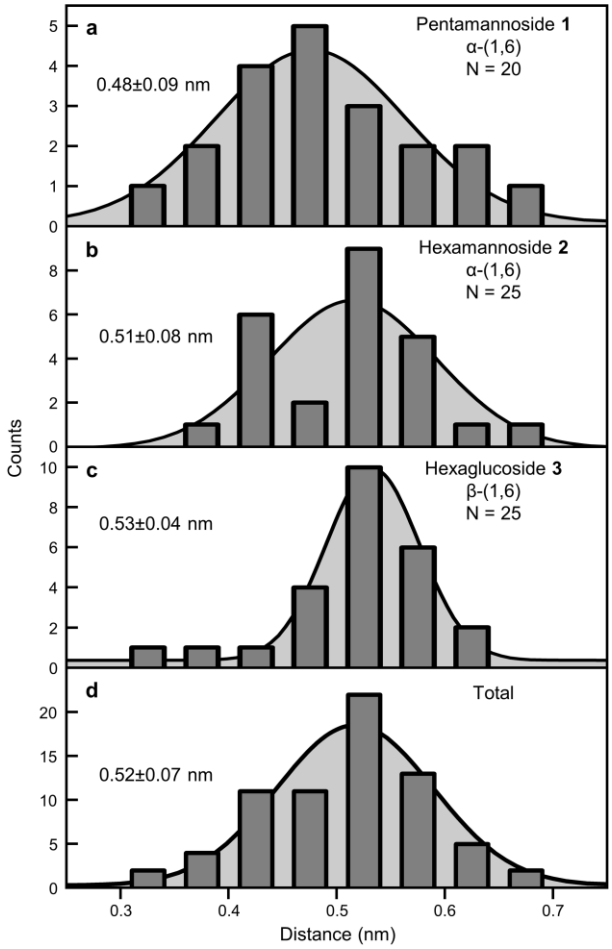

Figure 4ED | Statistical analysis of the features distance of (1→6) linkages in linear glycans. a, pentamannoside **1**, **b,** hexamannoside **2, c,** hexaglucoside **3. d,** Combined Histogram using all linear glycans. Values for mean feature distance of the (1→6) linkages were calculated by fitting with Gaussian peaks resulting in centre and width values of (0.48 ± 0.09) nm, (0.51±0.08) nm and (0.53±0.04) nm, respectively. The total averaging of the (1→6) linkages (including α-(1→6) and β-(1→6)) yields a measured 1-6 feature distance of (0.52±0.07) nm. Histogram bin size 0.05 nm.

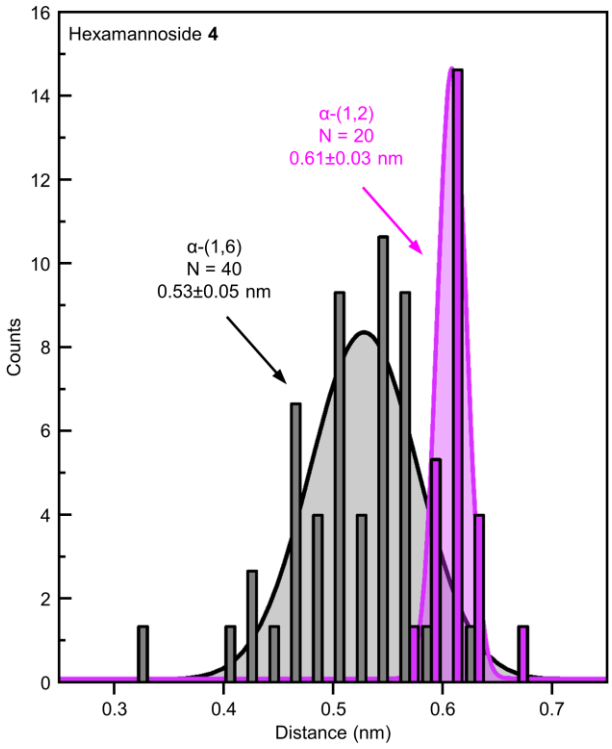

Figure 5ED | Statistical analysis of the feature distance of α-(1→6) and α-(1→2) linkages in hexamannoside 4. The distance between the monosaccharide units connected with α-(1→6) and α-(1→2) linkages in hexamannoside **4** was identified based on the linker position and the branching points. The histogram (bin size: 0.02 nm) of the α-(1→6) (gray) and α-(1→2) (purple) linkages was fitted with Gaussian peaks at (0.53±0.05) nm and (0.61±0.03) nm, respectively. The distributions show little overlap and thus the feature distance is identified as a reliable parameter to distinguish between α-(1→6) and α-(1→2) linkages. The wide distribution of α-(1→6) (black) linkages as compared to the narrow shape of α-(1→2) linkages (purple) hints towards larger conformational variability, likely due to the greater flexibility of the α-(1→6) links.

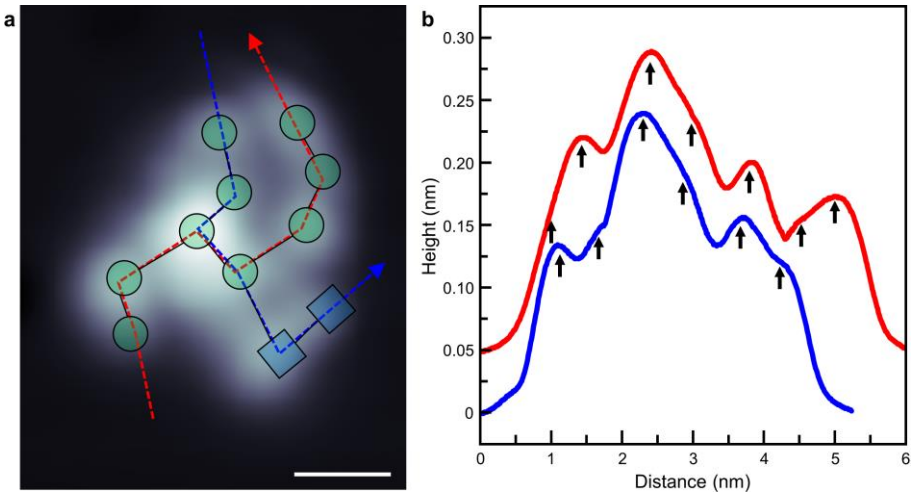

Figure 6ED | STM topography image of branched undecasaccharide 6. a, STM images of undecasaccharide **6,** clearly showing branching points and individually resolved monosaccharide units. The assignment of the branches is made by number of units in the branch and by the feature distance between the monosaccharide units. Scale bar: 1 nm**. b,** Line profiles as indicated in a.

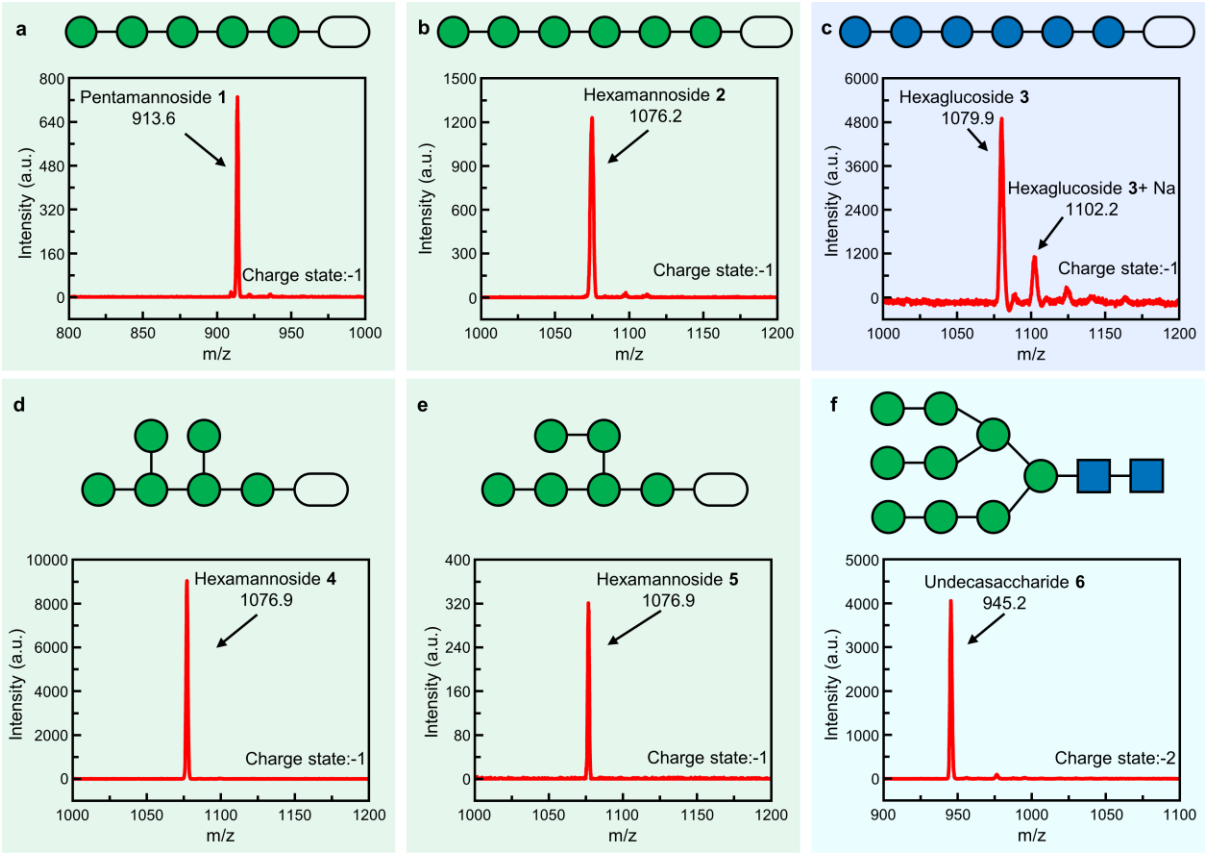

Figure 7ED | Mass spectra of all deposited glycans. The mass spectra show absence of major contaminants in the ion beam after mass filtering. For glycans **1-5,** the charge state of the molecule is -1, whereas the undecasaccharide **6** is has a charge state -2.